Preprints of the 19th World Congress
The International Federation of Automatic Control
Cape Town, South Africa. August 24-29, 2014

Energy Usage Simulation for 2 Articulated Robot Designs Having Stationary Motors and a Serial Robot Type Workspace

A.A. Shaik*. N. Tlale.**
G. Bright***

**Council for Scientific and Industrial Research, Pretoria, RSA (e-mail: ashaik@csir.co.za).*
***Anglo American PLC, Pretoria, RSA*
**** University of Kwa-Zulu Natal, Kwa-Zulu Natal, RSA*

Abstract: This paper discusses the design, modeling and energy usage simulation of 2 robotic manipulators. Both robots have a large workspace and are comparable to serial type robots, but their motor/gearbox pairs are held stationary at the robot base, and joint control is achieved by using concentric cylinder links and gears. Their energy usage is compared to a pure serial robot model to gauge if removing those motor/gearbox masses from the arm is in fact beneficial.

Keywords: Design, simulation, robot, energy, efficient.

1. INTRODUCTION

The serial robot architecture is widespread in modern day manufacturing. One disadvantage of the architecture is the location of motors and gearboxes which are either at the joint it controls or close by. Parallel robots save energy and increase speed when compared to serial robots due to the fact that they move less mass. A feature of this architecture is that the motor/gearbox pairs remain stationary while motion of an end effector is controlled by connected links, in closed loop architectures. Two questions then arose, would it be possible to keep all motors stationary on a machine design that could achieve the same workspace and dexterity as in a serial architecture, and would that design be more energy efficient?

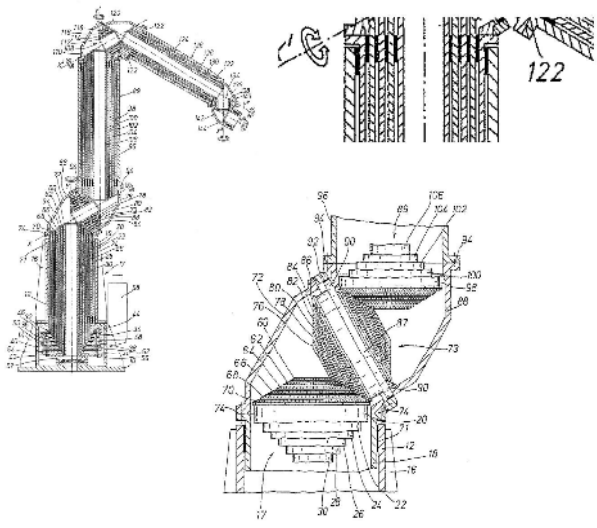

Fig. 1. Multi-articulated industrial robot from Bisiach (1989)

In the patent landscape only 2 designs were found. A European patent titled "Multi-articulated industrial robot with several degrees of freedom (DOFs) of movement", from Bisiach (1989) which described a robot that used hollow coaxial shafts and concentric geared mechanisms. This design had 7 DOFs, 3 DOFs to orient the tool and 4 DOFs to position it. Additionally no recent papers were found that discussed similar designs and energy usage.

Another German patent, "Robot arm with multiple links has drive transmitted to links from individual motors through coaxial shafts", from Pozzi (1989) also described a robot that used coaxial shafts and concentric geared mechanisms. This design also had 7 DOFs, with 3 for the orientation of a wrist and 4 to position the wrist centre. The gripper motor was also positioned at the base, but that did not constitute a robot DOF.

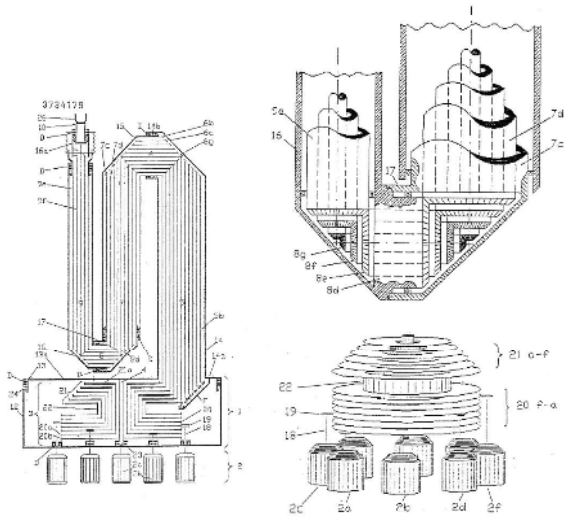

Fig. 2. Robot arm with multiple links and coaxial shafts from Pozzi (1989)

These 2 patents were most applicable as they had more than 6 DOFs and could achieve the same workspace but with greater dexterity (these were redundant robots). Both designs were forced to use a 2 DOF elbow joint to achieve the same motion trajectory as a serial robot, since the geared mechanisms at the elbow were set at 45º. 6 DOF serial robot designs have a 2-1-3 structure, that is 2 DOFs at the shoulder, 1 DOF at the elbow and 3 DOFs at the wrist. The patents mentioned were both 2-2-3 designs.

Other than the patents there was no supporting literature that either favoured the designs or warned against its implementation. The main contribution of this paper thus focuses on addressing this issue from an energy perspective.

2. SIMULATION METHOD

The designs by Pozzi (1989) and Bisiach (1989) were very similar, and a single simplified dynamic model representing both was used in the comparative simulations against a simplified serial robot. This model will be referred to as the PB model, although it refers to both patents. The simplification maintained the essence of the designs but ignored working detail. As mentioned previously the actual designs had 2 DOF elbow joints, so there were 5 concentric torque transfer cylinders on the proximal link plus the outer structural cylinder; and there were 3 concentric torque transfer cylinders on the distal link plus its outer structural cylinder. For motion comparison however the elbow joint was reduced to a single DOF whose axis was always parallel to the horizontal plane. This permitted reuse of the serial kinematic model already developed.

Essentially this model would produce dynamic results that were slightly better than the original design, since it didn't rotate one of the components (2 of the cylinders were fused together). For additional details on the modelling please see Shaik (2012). The simplified dynamic model is shown in fig. 3.

The torque of each joint is calculated in the machine level dynamics simulation where the coordinate origin of the end effector follows a time stamped path profile. A standard recursive dynamics algorithm can be found in Craig (2005). The algorithm requires the following data for implementation: joint angles for each pose along the path indicated, joint angular velocities and accelerations, robot model parameters which include inertia tensors, masses, centre of mass (COM) locations, velocities and accelerations. The work done by the robot is used as a measure of energy consumption which is given by the cumulative sum of joint work, for all joints at each pose along the path. Joint work is the multiplication of torque applied at the joint and the angular displacement it induces.

For the purpose of the objective set out in this research, only the work done in translation of the end effector was of interest. The wrist was not controlled in any specific way and work done in orientation of the wrist was thus not considered for any of the models. For the robot design a large number of parameters could vary, taking into account all would not be practical, and for this reason one parametric model was used for the Pozzi and Bisiach designs.

The serial robot model however had mass from its wrist, elbow and shoulder motors which it had to move, and for that 2 parametric models were used to highlight the effect of motor mass. The models used low mass (LM) and high mass (HM) motors respectively, and it was assumed that the motors would have sufficient ability to move as required in the path specification. Motor mass was taken as a percentage of all the mass it moved, and for low and high mass motors this was set at 4% and 35% respectively.

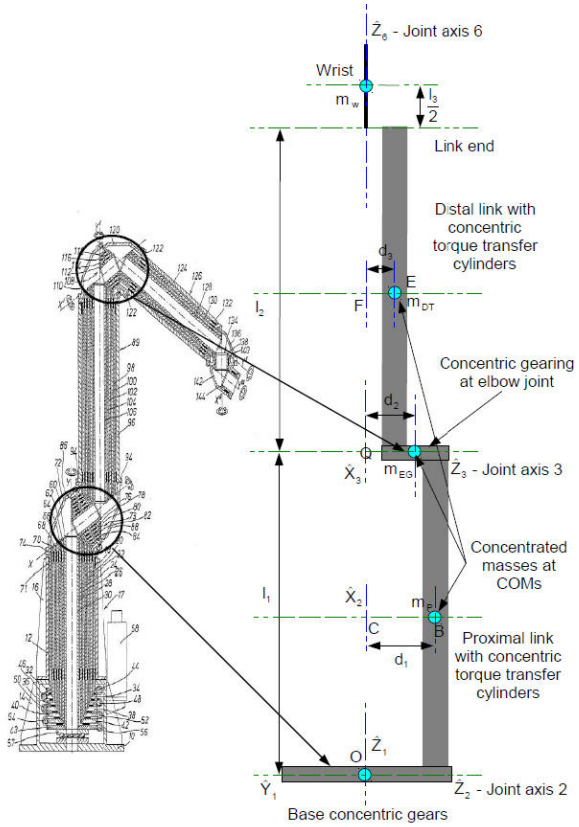

Fig. 3. Simplified modelling for dynamics implementation of Pozzi and Bisiach designs taken from Shaik (2012)

The motor geometry was modelled as a block with varying edge length, whose density was estimated at 15% steel, 40% ferrite, 40% copper and 5% empty space, i.e. 6709.5 kg.m^{-3}. The density was essential to derive motor volume and the side lengths or edges were calculated from parametric relations between the edges. In total the motor mass for the light version of the serial robot was an additional 8.15% more than that for the new design. For the heavy version of the serial robot it was 70.8% heavier.

The simulations were carried at 2 speeds, the first being very slow so that the dynamic response of the machine was close to its static state. This meant that the torques required for motion were slightly larger than that required to maintain a static pose. The second speed was excessive and may not be physically achievable but it was necessary to illustrate how the robot models compared with each other when the dynamic response was dominant. For each path the end-

effector followed a simple velocity profile. It started at the beginning of the path with 0m.s^{-1} velocity, and accelerated with constant positive acceleration to a maximum, after which it ramped down to 0m.s^{-1} with constant negative acceleration. There must be a finite duration between changes in acceleration in real world situations, and so the acceleration graph should be an S-curve instead of a straight edged step curve. Since the derivative of acceleration was never used, that bit of real world detail was ignored. The velocity graph has straight lines, and the distance graph has an S shape.

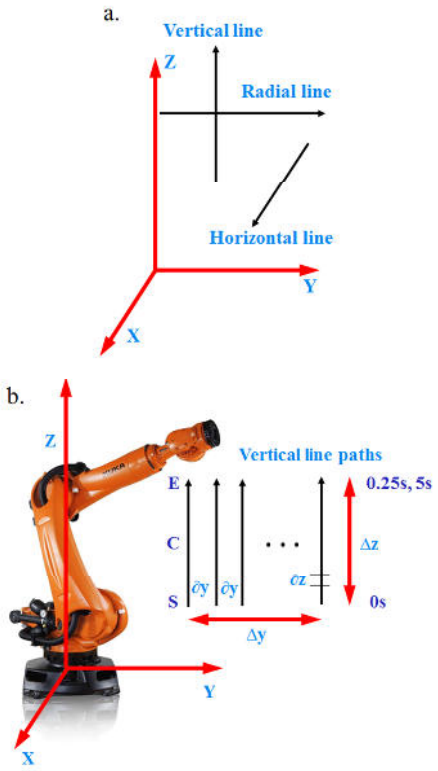

Fig. 4. Illustration of straight line paths

A robot's work path could have a large number of segments either linear or curved which are connected in an infinite number of ways. It was decided to compare the dynamics over the simplest comprising elements of a complex path. These were straight line segments and circular curves. The straight line paths were vertical, horizontal and radial. Vertical lines were perpendicular to the xy plane, radial lines were perpendicular to the z axis and parallel to the xy plane, and horizontal lines were perpendicular to both vertical and radial lines. Any other line path could be considered as a linear combination of the above paths, i.e. a diagonal line would be composed of a horizontal line with a vertical or a radial line with a vertical line, etc. For each straight line path type the dynamics were tested over a range of lines. This is illustrated in fig. 4b for vertical line paths, and the discussion is the same for horizontal and radial paths. The vertical lines have the same length given by Δz, and are specified by the Start, Centre and End (SCE) coordinates. Motion for the vertical paths would start at S and end at E, with a path increment of ∂z. Once a path completes the y coordinate is incremented by ∂y to move onto the next path. The robot then traces that path from S to E incrementing the z coordinate only. This continues until the last vertical path is reached where the total change in y coordinate from the first to the last vertical path is Δy. This is done at 2 speeds first very slow, with a total path time of 5s and then very fast with a total path time of 0.25s. The straight line path profiles are captured in table 1.

Only the total energy consumed at the end of each path was taken, which was plotted against the coordinate that was advanced (the y value for the vertical and horizontal paths; and the z value for the radial paths).

Table 1. Straight line path specification

Path	SCE (m)	Variable coordinate (m)
Vertical lines ($\Delta z = 1.066$)	$\begin{bmatrix} 0 & 0 & 0 \\ y_i & y_i & y_i \\ 0.213 & 0.746 & 1.280 \end{bmatrix}$	$0.32 \le y_i \le 1.706$ $\Delta y = 1.386$ $\partial y = 0.035$
Horizontal lines ($\Delta x = 1.066$)	$\begin{bmatrix} -0.533 & 0 & 0.533 \\ y_i & y_i & y_i \\ 0.746 & 0.746 & 0.746 \end{bmatrix}$	$0.32 \le y_i \le 1.706$ $\Delta y = 1.386$ $\partial y = 0.035$
Radial lines ($\Delta y = 1.066$)	$\begin{bmatrix} 0 & 0 & 0 \\ 0.213 & 0.746 & 1.280 \\ z_i & z_i & z_i \end{bmatrix}$	$0.533 \le z_i \le 1.599$ $\Delta z = 1.066$ $\partial z = 0.027$

For the circular paths it was decided to isolate the first 3 axes responsible for wrist centre translation, i.e. only 1 of those 3 angles would change while the remaining 5 were kept constant. This allowed the wrist centre to move on a circular arc about the actuated axis. Angles 1 to 3 control the orientation about axes $\hat{Z}_1$ to $\hat{Z}_3$ in fig. 3 respectively.

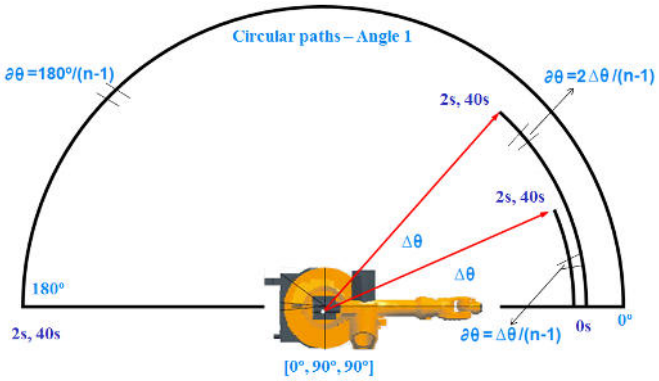

Fig. 5. Illustration of circular path specification for angle 1

Additionally this resulted in a large change in joint angle (difference between the start and end angular positions), unlike in the straight line paths. Each circular path, for each axis had a common start angle, which was given relative to that joint's coordinate frame axis. The end angle was varied between selected minimum and maximum values, with the increment given by $\Delta\theta$.

The increment in each path was given by $\partial\theta$. The circular path specifications for angle 1 are illustrated in fig. 5 and are given in table 2. In the table variable m sets the number of paths in the angular range for a joint, and variable n sets the angular resolution for a particular path. Again the dynamics for each model was tested at 2 different speeds (slow then fast). For each of these 3 axes the arm was tested at the best and worst case mass moments about the individual axes, which would give the lowest and highest joint torque respectively. The worst moments are achieved when the arm mass is at its furthest location from the axis being tested, and the best case was the opposite. For rotation about the vertical z axis the worst case is when the arm points out and is perfectly horizontal, where the distal and proximal links are parallel. The best case is achieved when the arm points up vertically, and again both links are parallel. Those were singularity conditions but the aim was to move the wrist centre on the workspace boundary. There are similar cases for the remaining shoulder and elbow joint (axes 2 and 3).

Table 2. Circular path specification

Angle varied	Arm config. $[\theta_1 \quad \theta_2 \quad \theta_3]$; $[\theta_4 \quad \theta_5 \quad \theta_6] = [0° \quad 0° \quad 0°]$	Range $2 \le k \le m;\ m \ge 2$ $1 \le i \le n;\ n \ge 2$
Angle 1	$[\theta_{1(i)} \quad 0° \quad 0°]$	$\Delta\theta = \frac{180°}{m-1}$ $\Delta\theta \le \theta_{1(k)} \le 180°$ $\theta_{1(k+1)} = \theta_{1(k)} + \Delta\theta$ $\partial\theta = \frac{\theta_{1(k)}}{n-1}$ $\theta_{1(n)} = \theta_{1(k)};\ \theta_{1(1)} = 0°$ $0° \le \theta_{1(i)} \le \theta_{1(n)}$ $\theta_{1(i+1)} = \theta_{1(i)} + \partial\theta$
	$[\theta_{1(i)} \quad 90° \quad 0°]$	
Angle 2	$[0° \quad \theta_{2(i)} \quad 0°]$	$\Delta\theta = \frac{90°}{m-1}$ $\Delta\theta \le \theta_{2(k)} \le 90°$ $\theta_{2(k+1)} = \theta_{2(k)} + \Delta\theta$ $\partial\theta = \frac{\theta_{2(k)}}{n-1}$ $\theta_{2(n)} = \theta_{2(k)};\ \theta_{2(1)} = 0°$ $0° \le \theta_{2(i)} \le \theta_{2(n)}$ $\theta_{2(i+1)} = \theta_{2(i)} + \partial\theta$
	$[0° \quad \theta_{2(i)} \quad 170°]$	
Angle 3	$[0° \quad 0° \quad \theta_{3(i)}]$	$\Delta\theta = \frac{180°}{m-1}$ $-90° + \Delta\theta \le \theta_{3(k)} \le 90°$ $\theta_{3(k+1)} = \theta_{3(k)} + \Delta\theta$ $\partial\theta = \frac{\theta_{3(k)}}{n-1}$ $\theta_{3(n)} = \theta_{3(k)};\ \theta_{3(1)} = -90°$ $-90° \le \theta_{3(i)} \le \theta_{3(n)}$ $\theta_{3(i+1)} = \theta_{3(i)} + \partial\theta$

3. MULTI-STRAIGHT LINE PATH SIMULATION RESULTS

The graphs for the PB model are relative to the serial robot, and are displayed as a percentage thereof for both cases. The dash double dot and solid lines represent the low and high dynamics cases respectively for comparison against the low mass (LM) and high mass (HM) serial robot models.

a. Energy used on vertical line paths (LM)

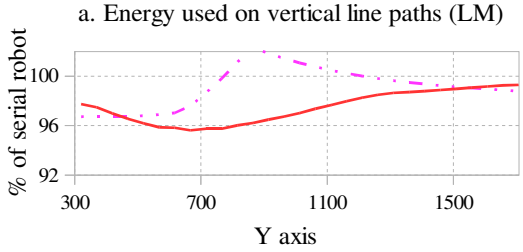

b. Energy used on vertical line paths (HM)

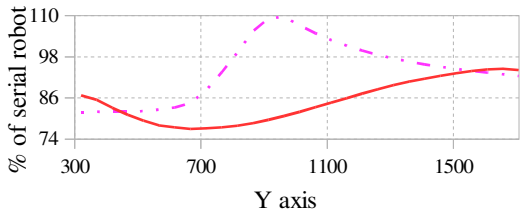

c. Energy used on horizontal line paths (LM)

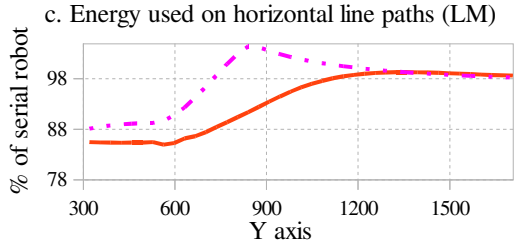

d. Energy used on horizontal line paths (HM)

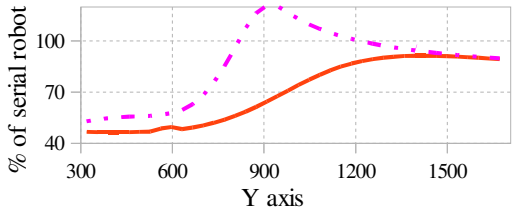

e. Energy used on radial line paths (LM)

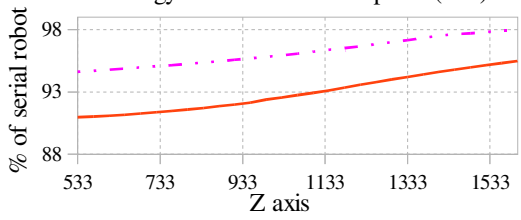

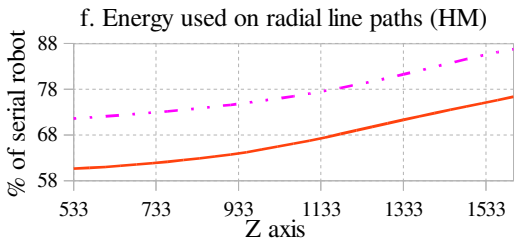

Fig. 6. Total energy consumption data for multiple vertical, horizontal and radial line paths

4. CIRCULAR PATH SIMULATION RESULTS

The simulation results presented here were a comparison of total energy usage only (total energy consumed per model at the end of each circular path), and is illustrated in table 3. The tabular form is due to the fact that the percentage energy comparison against the serial robot for these paths and joint constraints were either constant throughout the range of motion or varied very slightly.

Table 3. Circular path energy usage results

			% Energy usage	
Angle varied	Arm config.	Serial robot model	Low speed (40s)	High speed (2s)
Angle1	θ_2=0º, θ_3=0º	LM	97.14	97.14
		HM	82.98	82.98
	θ_2=90º, θ_3=0º	LM	100.2	100.18
		HM	45.02	45.01
Angle 2	θ_1=0º, θ_3=0º	LM	95.69	95.69
		HM	77.22	77.24
	θ_1=0º, θ_3=170º	LM	89	89.02
		HM	55.39	55.45
Angle 3	θ_1=0º, θ_2=0º	LM	100.55	100.56
		HM	103.48	103.49

5. CONCLUSIONS

The data indicates that in most cases and majority of the paths the PB model should be more energy efficient than a serial robot even when the serial robot's motor mass is low. During some parts in the vertical and horizontal line path motion of the low dynamics case the serial robot was more energy efficient, which included the high motor mass case. When the robot moves fast however the Pozzi and Bisiach designs should use less energy in every case.

The PB model performed better when rotating angles 1 and 2 only (except the config. where the arm points vertically up against the LM serial robot model) in the circular path motion. At higher speeds there was a larger saving when compared to the HM serial robot. The situation was different for the elbow joint also known as axis 3. Here even though the serial robot was moving more mass there was a more significant balancing effect at that joint. This effectively brought the mass moment of that link closer to the axis and lowered its overall energy usage.

In conclusion a design that forces a static location of motor/gearbox pairs in a large workspace, articulated arm type structure can save energy, and in the long term it will be significant. The static balancing effect of a typical serial robot however is important and it should be applied to the new design to bring about an additional drop in energy usage. This will be investigated further.

When weighed against the complicated nature of the Pozzi and Bisiach designs, as well as any maintenance and repairs that would have to be performed, the amount of energy saved may not be sufficiently enticing to demand implementation.

REFERENCES

Bisiach, B., (1989). Multi-articulated industrial robot with several degrees of freedom of movement, patent number: 0299551A1.

Pozzi, U., (1989). Robot Arm with Multiple Links has Drive Transmitted to Links from Individual Motors through Coaxial Shafts, patent number: DE3734179A1.

Shaik, A.A., (2012). Design, modelling and simulation of 2 novel 6 DOF hybrid machines, PhD thesis (UKZN).

Craig, J.J., (2005). *Introduction to robotics, mechanics and control*, Pearson Education.